WEP Warwick Evans Publishing

Journal of Educational Development and Social Sciences

ISSN: 3080-9967 (Print), ISSN: 3080-9975 (Online)
Volume 1, Number 6, Year 2026
DOI: https://doi.org/10.62051/jedss.v1n6.03



Image Enhancement Method based on 1:1 Resonant Hopf Bifurcation in Time-Delay Neural Networks

Mingrui Wang*, Kaiwen Wang, Chenglong Wang, Zhihao Xiang, Mingjun Yang, You Wu

School of Artificial Intelligence, China University of Mining and Technology (Beijing), Beijing 100083, China

*Corresponding Author: Mingrui Wang (Email: wang_m_r@163.com)

ABSTRACT

This paper investigates the 1:1 resonant Hopf bifurcation characteristics of a class of time-delay neural network models and their application in low-light image enhancement. By analyzing the characteristic equation of the linearized system, the conditions for the asymptotic stability of the equilibrium point and the critical delay for the Hopf bifurcation are derived. It is further obtained that at the critical delay, the system undergoes a 1:1 resonant Hopf bifurcation, and the amplitude of the periodic solution grows at a rate of $\mu^{\frac{1}{6}}$. Based on this amplitude amplification mechanism, a time-delay neural network image enhancement algorithm is constructed: the pixel values of the low-light image are assigned as the initial values of neuron u_1, and contrast enhancement is achieved by utilizing the periodic solution outputs of neuron u_2 or u_3 through the selection of appropriate delay parameters and evolution time t. Experiments were conducted using 10 real low-light images from the LIME dataset, and quantitative comparisons were made with the linear grayscale enhancement method and the gamma transformation method. The results indicate that the proposed algorithm significantly outperforms the comparison methods in terms of image mean, standard deviation, and information entropy, effectively improving image brightness, contrast, and detail richness. It performs moderately on the NIQE index, suggesting a compromise in naturalness when intensely stretching the grayscale range, yet the overall enhancement performance remains outstanding. This paper provides a new approach with a clear mathematical mechanism for image enhancement.

KEYWORDS

Time-delay neural network; 1:1 resonance; Hopf bifurcation; Low-light image enhancement.

1. INTRODUCTION

As one of the most important carriers for humans to perceive the world and acquire information, images play an irreplaceable role in the development of modern technology and society. With the rapid development of fields such as artificial intelligence, remote sensing and mapping, biomedical engineering, intelligent manufacturing, and security surveillance, the requirements for image quality have been continuously increasing. For instance, remote sensing images require clear presentation of surface details to support resource surveys and disaster warning; medical CT/MRI images rely on high contrast to achieve accurate lesion identification; industrial vision systems need noise-free, highly detailed images for precision component quality inspection; and security surveillance requires the extraction of effective visual information under low-light and complex environments [1-3]. Constrained by the performance limitations of imaging devices, insufficient lighting conditions, or signal attenuation during transmission, original images often suffer from quality issues such as low contrast, blurred edges, and loss of detail information, which severely affect the accuracy of

Content from this work may be used under the terms of CC BY-NC 4.0 licence (https://creativecommons.org/licenses/by-nc/4.0/).
Published by Warwick Evans Publishing.

subsequent analysis and recognition tasks [4-6]. Therefore, as a fundamental step in image processing, image enhancement aims to improve visual effects and enhance the interpretability and usability of images through specific technical means, possessing significant theoretical value and practical significance.

Traditional image enhancement methods can be divided into two main categories: spatial domain methods and frequency domain methods. However, they generally suffer from over-reliance on global statistical information of the image, difficulty in adaptively processing detail differences in various local regions, and a tendency to introduce noise or over-enhancement. Consequently, their enhancement effects are often unsatisfactory in complex and variable visual environments [7-8].

In recent years, nonlinear dynamical system theory has demonstrated unique advantages and broad application prospects in the field of image processing. Morfu and Comte first proposed the use of a nonlinear oscillator network for image contrast enhancement, theoretically and numerically demonstrating that the contrast of grayscale images can be significantly enhanced even if the initial value is very small[9]. Morfu further extended the nonlinear oscillator network to a cellular nonlinear network, achieving multiple functions such as contrast enhancement, video inversion, and grayscale extraction without the need to reconfigure the network structure [10]. On this basis, a new image filtering algorithm inspired by diffusion processes was further proposed, indicating that a pure nonlinear diffusion process can achieve contrast enhancement and noise filtering while generating a certain degree of image blur. Combining the characteristics of anisotropic diffusion and nonlinear diffusion can yield better processing results [11].

As typical nonlinear dynamical systems, time-delay neural networks possess rich dynamical behaviors, including equilibrium stability, bifurcations (such as Hopf bifurcation and resonant bifurcation), and periodic solution evolution. These provide interpretable and tunable mathematical mechanisms for image processing[12]. Golubitsky's research indicated that within the critical bifurcation region where symmetry breaking occurs in feed-forward networks, the center manifold of the system completely inherits the feed-forward topological structure of the original network. Relying on this core structural characteristic, relevant theories have further confirmed the existence of periodic solution branches near such bifurcation points, and the amplitude of the periodic solutions grows at a specific rate of $\mu^{\frac{1}{6}}$ [13-14]. By means of such unique dynamical behaviors, precise detection and effective amplification of weak signals with specific frequencies in natural environments can be achieved, thereby providing a novel dynamical implementation path for signal enhancement and feature extraction.

2. DYNAMICAL ANALYSIS OF A TIME-DELAY NEURAL NETWORK MODEL

To reveal the resonant amplification mechanism of time-delay neural networks, a class of 5-dimensional feed-forward time-delay neural network model is constructed in this section. Through linearization analysis, the critical conditions for its Hopf bifurcation and 1:1 resonance are derived.

$$\begin{cases} \dot{u}_1 = -u_1 + (a+b)\tanh(u_1(t-\tau)), \\ \dot{u}_2 = au_2 - {u_2}^3 - v_2 + a\tanh(u_1(t-\tau)), \\ \dot{v}_2 = u_2(t-\tau) - bv_2, \\ \dot{u}_3 = au_3 - {u_3}^3 - v_3 + a\tanh(u_2(t-\tau)), \\ \dot{v}_3 = u_3(t-\tau) - bv_3. \end{cases} \tag{1}$$

In model (1), except for the first neuron unit, each subsequent layer of neurons is driven by the dynamical output of the preceding neurons. As the system state evolves over time, this multi-layer coupled feed-forward chain model can exhibit asymmetric resonant dynamical phenomena.

It is easy to see that $(0,0,0,0,0)$ is the equilibrium point of model (1). By linearizing model (1) at the zero equilibrium point, the characteristic equation of the linearized system is obtained as:

$$f(\lambda) = \Delta_1 \Delta_2^2 \tag{2}$$

Where: $\Delta_1 = \lambda + 1 - (a+b)e^{-\lambda\tau}, \Delta_2 = \lambda^2 + (-a+b)\lambda - ab + e^{-\lambda}$.

When $0 < a < b$ and $a + b < 1$, all roots of $\Delta_1 = 0$ have strictly negative real parts, so we only need to consider $\Delta_2 = 0$. It is easy to see that when $\tau = 0$, the roots of $\Delta_2 = 0$ have strictly negative real parts. Let $\lambda = i\omega(\omega > 0)$ be a root of the equation $\Delta_2 = 0$. Substituting it into the equation yields:

$$(\omega^2 + ab)^2 + \omega^2(b-a)^2 = 1 \tag{3}$$

Simplifying this gives:

$$\omega = \sqrt{\frac{-(a^2+b^2)+\sqrt{(a^2+b^2)^2-4(a^2b^2-1)}}{2}} \tag{4}$$

Consequently:

$$\tau_j = \frac{1}{\omega}(arccos(\omega^2 + ab) + 2j\pi), (j = 0,1,\cdots) \tag{5}$$

According to reference [15], the zero equilibrium point is asymptotically stable.

Calculating the transversality condition:

$$Re\left(\frac{d\lambda}{d\tau}\right)^{-1}\Big|_{\tau=\tau_j} 2\omega(\omega^3 + (b-a)\omega^2) + ab(b-a) > 0. \tag{6}$$

By utilizing the bifurcation theory of functional differential equations, it is obtained that: there exists $\tau = \tau_j(j = 0,1,\cdots)$ such that when $\tau \in (0, \tau_0)$, the zero equilibrium point is asymptotically stable; and when $\tau = \tau_j(j = 0,1,\cdots)$, the system undergoes a Hopf bifurcation at the zero equilibrium point, where $\tau = \tau_j(j = 0,1,\cdots)$ is determined by the characteristic equation $f(\lambda) = \Delta_1\Delta_2^2$.

From the characteristic equation (2), it can be seen that at $\tau = \tau_j$, there is a pair of pure imaginary roots $\pm i\omega$ with an algebraic multiplicity of 2 and a geometric multiplicity of 1. According to reference [16], model (1) can undergo a 1:1 resonant Hopf bifurcation. Under the action of the resonance mechanism, the amplitude of the periodic solution corresponding to the periodically

moving neurons grows at a rate much faster than that in the ordinary bifurcation case. Applying this characteristic to image enhancement can yield satisfactory enhancement effects.

3. NUMERICAL SIMULATION AND IMAGE ENHANCEMENT EXPERIMENTS

This section demonstrates the evolution behavior of the system's periodic solutions through numerical simulations and constructs an image enhancement algorithm based on this resonant amplification mechanism.

3.1 Dynamical Numerical Simulation and Phase Difference Analysis

The parameters were set as $a = 0.2$ and $b = 0.5$, satisfying the conditions $0 < a < b$ and $a + b < 1$. By substituting these into equations (4) and (5), the critical frequency $\omega = 0.927630$ and the critical delay $\tau_0 = 0.304014$ were calculated. To induce the 1:1 resonance, the delay parameter was selected as $\tau = 0.85 > \tau_0$, and the evolution state of each neuron in system (1) over time was observed. As shown in Fig. 1, neurons u_2, v_2, u_3 and v_3 undergo a 1:1 resonant Hopf bifurcation and exhibit periodic oscillations, which provides a dynamical foundation for amplifying the input signal of neuron u_1.

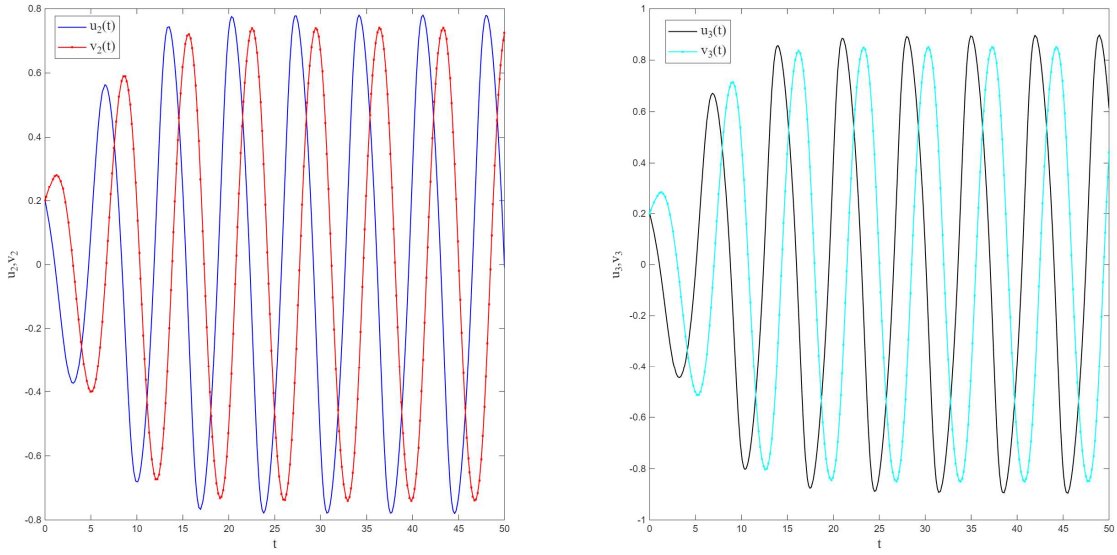


Figure 1. Periodic solutions of neurons u_2, v_2, u_3 and v_3 $(\tau = 0.85 > \tau_0)$

When the system undergoes a 1:1 resonant Hopf bifurcation, all subsequent neurons enter a state of periodic oscillation. However, the periodic oscillations of these neurons are not completely synchronized in time with those of the preceding neurons. This temporal offset in oscillation rhythm manifests as the phase difference between the neurons. In the amplitude amplification mechanism of the 1:1 resonance, the phase difference is a crucial parameter. When the phase difference between the output neuron and the input neuron reaches its peak, it indicates that the subsequent neuron is at an extreme state (i.e., wave crest or trough). At this moment, the stretching (amplification) effect on the input signal is most significant.

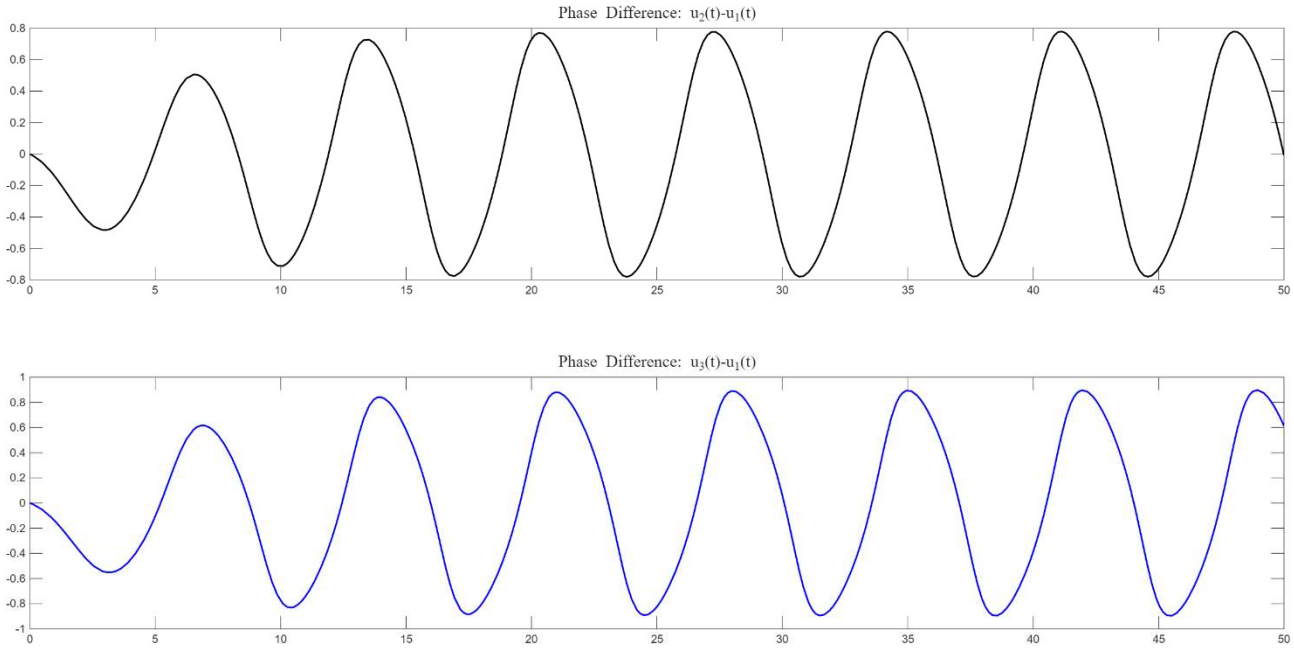


Figure 2. Phase difference of neurons u_2, u_3 and neurons u_1 ($\tau = 0.85 > \tau_0$)

Figure 2 illustrates the phase differences between neurons u_2, u_3, and u_1 at different times. At $t = 5.55432$, the phase difference between neuron u_2 and u_1 is greater than that between u_3 and u_1; at $t = 6.53035$ and $t = 13.8471$, the phase difference between neuron u_2 and u_1 is smaller than that between u_3 and u_1; and at $t = 13.8471$, the phase difference between neuron u_3 and u_1 reaches a relative maximum. The phase differences between neurons u_2, u_3, and u_1 exhibit periodic fluctuations over time. Under the 1:1 resonance mechanism, the magnitude of the phase difference directly determines the amplification capability of the subsequent neurons on the preceding signal. A larger phase difference implies that the response of the subsequent neuron can better avoid the wave trough of the preceding signal, thereby driving the signal amplitude to a higher level through the coupling effect.

3.2 Visual and Histogram Analysis of Low-contrast Image Enhancement

In image enhancement experiments, the histogram is one of the most intuitive and commonly used statistical tools for evaluating the enhancement effect. The histogram of a low-contrast image typically exhibits an extremely narrow grayscale distribution, concentrated within a small low-intensity interval. Conversely, for an effectively enhanced image, the dynamic range of its histogram expands significantly, and the grayscale distribution becomes more balanced, thereby visually presenting higher contrast and richer details.

Figure 3 shows the Lena low-contrast image and its histogram, with pixel values in the range of $[0,0.2]$. The pixel values of this low-contrast image were input as the initial values of neuron u_1 in model (1). Through the continuous evolution of model (1), neuron u_2 (or u_3) could amplify the input signal of neuron u_1 via the coupling effect. By taking the values of neuron u_2 (or u_3) as the output values, the image enhancement effect was achieved. Figures 4 to 6 show the image enhancement effects with u_2 and u_3 as the output values at different times, respectively.

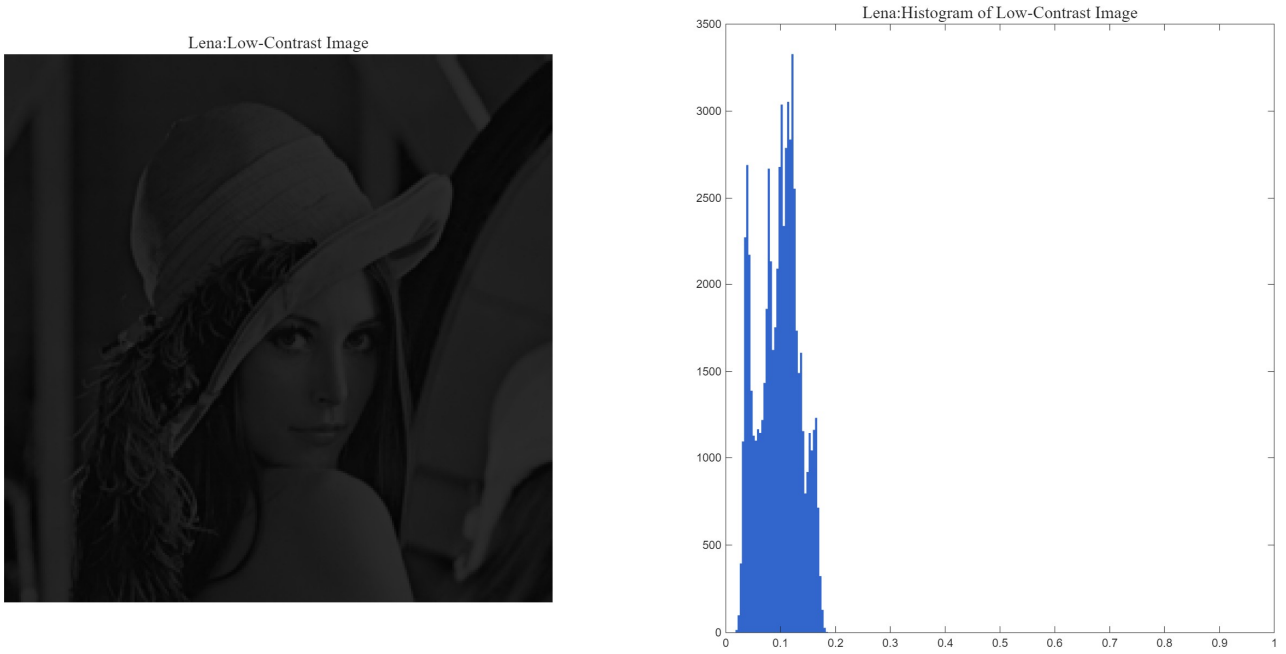


Figure 3. Lena low-contrast image and its histogram

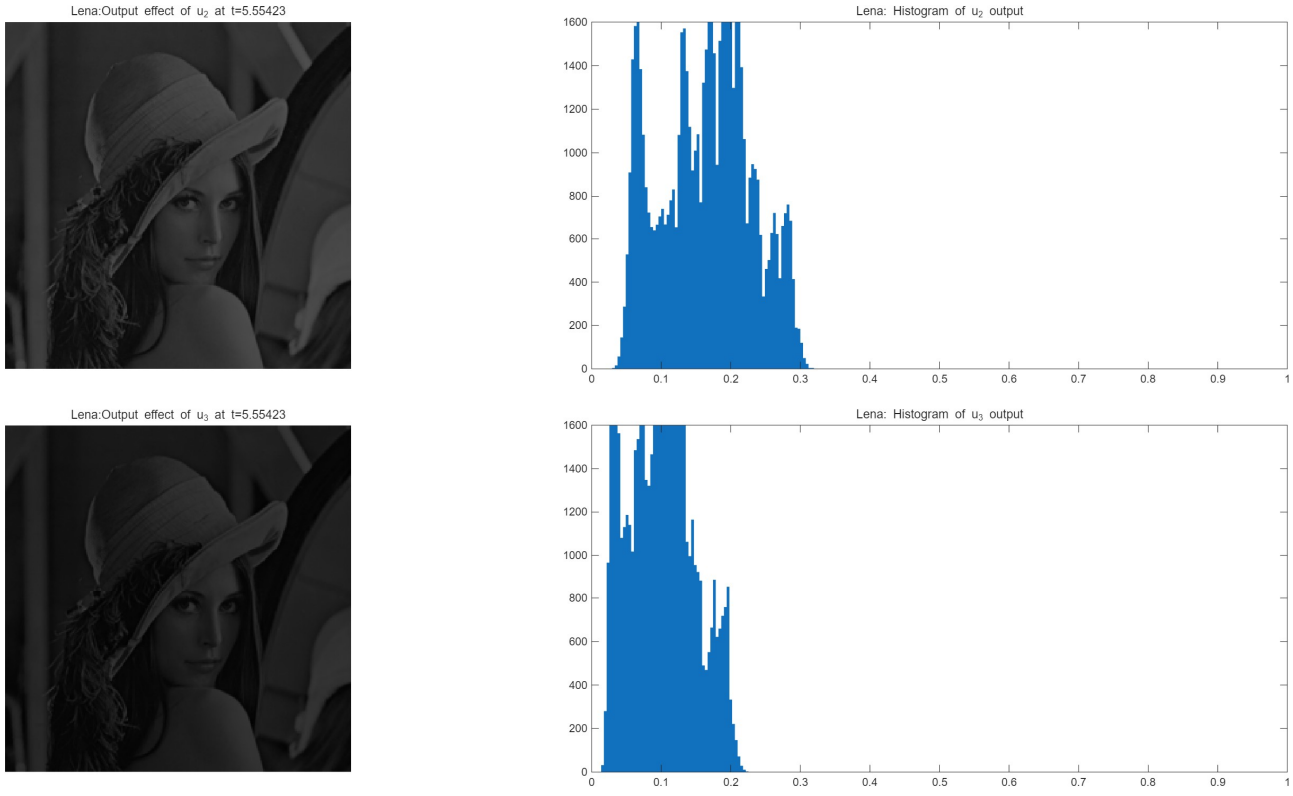


Figure 4. Image enhancement effects with neurons u_2 and u_3 as output values at $t = 5.55432$

At different values of time t, the enhancement effects produced by neurons u_2 and u_3 varied. At $t = 5.55432$, when the value of neuron u_2 was taken as the output, the histogram showed that the range of the output pixel values was expanded to $[0,0.325]$. At this time, when the value of neuron u_3 was taken as the output, the histogram indicated that the range of the output pixel values was expanded to $[0,0.231]$. Consequently, the enhancement effect of neuron u_2 was stronger than that of neuron u_3, which is consistent with the magnitude of the phase difference at $t = 5.55432$ shown in Figure 2.

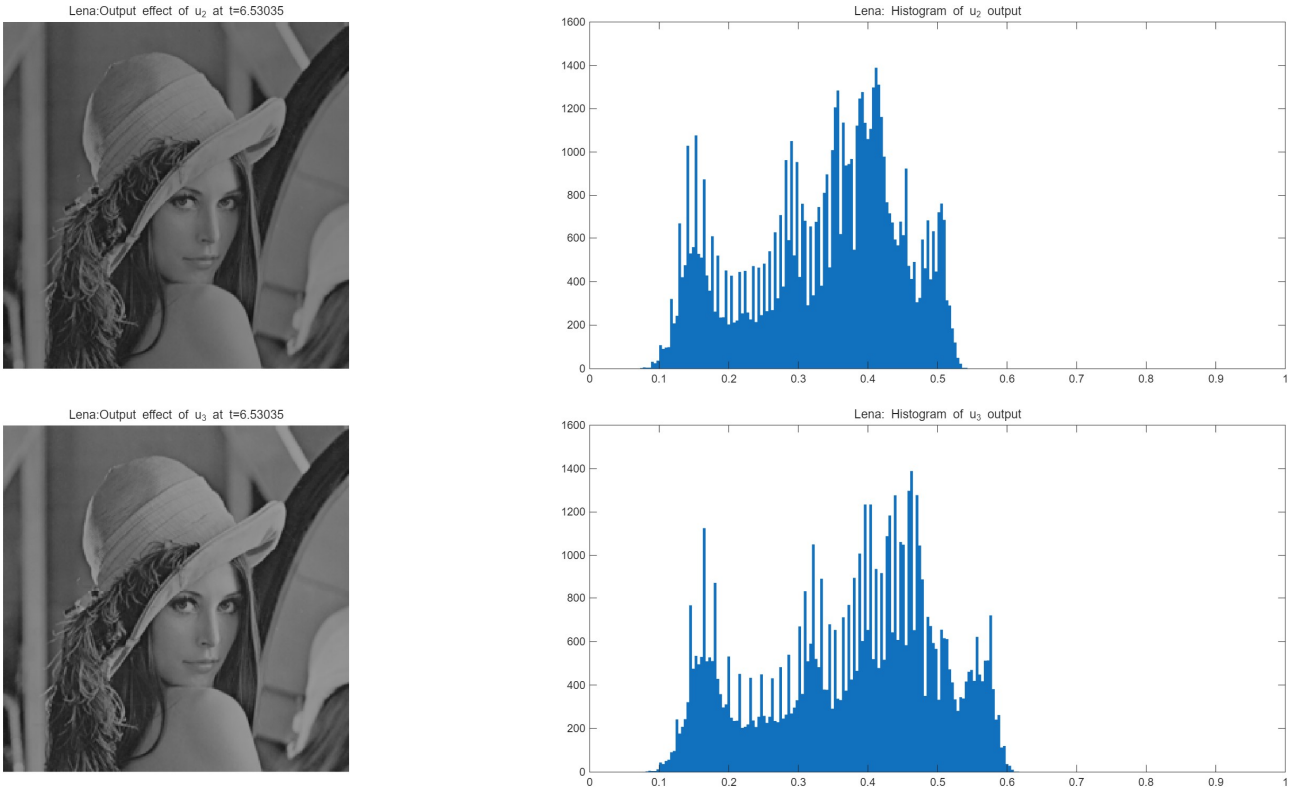


Figure 5. Image enhancement effects with neurons u_2 and u_3 as output values at $t = 6.53035$

Figure 5 shows the enhancement effects of neurons u_2 and u_3 at $t = 6.53035$. Neuron u_2 expanded the pixel value range to $[0,0.547]$, while neuron u_3 expanded the pixel value range to $[0,0.622]$. At this time, the enhancement effect of neuron u_3 was stronger than that of neuron u_2.

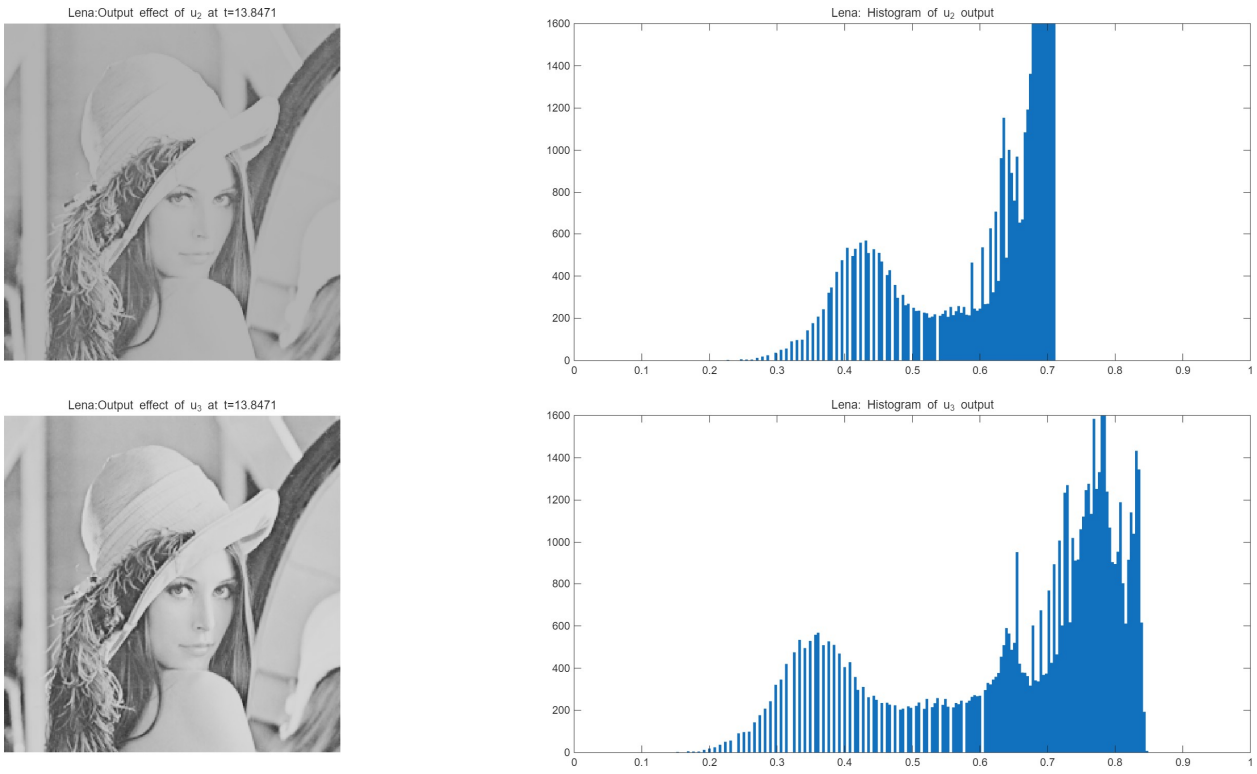


Figure 6. Image enhancement effects with neurons u_2 and u_3 as output values at $t = 13.8471$

Figure 6 shows that at $t = 13.8471$, the output pixel value range of neuron u_2 was expanded to $[0,0.710]$, and that of neuron u_3 was expanded to $[0,0.849]$. The enhancement effect reached a local optimum, which is consistent with the phase difference shown in Figure 2.

4. OBJECTIVE EVALUATION OF IMAGE ENHANCEMENT EFFECTS

The evaluation of image enhancement effects typically employs multiple objective metrics for comprehensive assessment, the core of which lies in measuring the visual presentation quality and detail preservation of the images. Commonly used evaluation metrics include image mean, standard deviation, information entropy, and the Natural Image Quality Evaluator (NIQE). These metrics provide a comprehensive and quantitative analysis of the image enhancement effects from multiple dimensions, such as brightness, contrast, and detail richness. They not only focus on the overall visual presentation of the image but also take local detail performance into account, providing a scientific basis for the quantitative evaluation of the enhancement effects [17].

In the field of image enhancement, the linear grayscale enhancement method and the gamma transformation method are two typical baseline methods. The linear grayscale enhancement method adjusts image contrast through linear mapping. It has the advantages of a simple principle and low computational complexity, making it suitable for basic brightness and contrast adjustments. However, it suffers from poor flexibility, struggles to balance local details, and is prone to amplifying noise. The gamma transformation method utilizes a nonlinear power function mapping, which better aligns with human visual characteristics. It can specifically optimize dark (or bright) details and is widely applied in scenarios such as low-light and medical imaging. Nevertheless, the core parameter of this method, the gamma coefficient, usually relies on empirical manual selection, exhibiting weak adaptive capability.

To verify the effectiveness and advancement of the time-delay neural network image enhancement algorithm proposed in this paper, 10 real low-light images from the unsupervised Low-Light Image Enhancement dataset (LIME) were selected as test samples in this section. The LIME dataset covers various complex lighting scenes, such as night street views and dark buildings, and lacks corresponding normal-light reference images, making it a typical no-reference benchmark dataset. This imposes higher requirements on the algorithm in terms of brightness improvement, contrast enhancement, and noise suppression.



Figure 7. Low-light images from the LIME dataset



Figure 8. Results of image enhancement processed by the time-delay neural network model

In this section, the proposed algorithm was compared with the linear grayscale enhancement method and the gamma transformation method, and a quantitative analysis was conducted based on four objective evaluation metrics: image mean, standard deviation, information entropy, and NIQE.

4.1 Image Mean Comparison

The image mean refers to the arithmetic average of the grayscale values of all pixels in an image, which directly reflects the overall brightness of the image. A larger mean value corresponds to a brighter image, whereas a smaller mean value indicates a darker image. The primary objective of low-light image enhancement is to improve dark environments. By comparing the image means processed by different algorithms, the capability of each algorithm to enhance overall image brightness can be objectively evaluated.

Table 1. Image Mean Comparison

Image	Linear grayscale enhancement method	Gamma transformation method $\boldsymbol{\gamma = 0.5}$	Gamma transformation method $\boldsymbol{\gamma = 1}$	The proposed algorithm
Image 1	60.3718	45.3823	10.4033	**74.6059**
Image 2	61.0278	48.2305	11.0490	**89.5638**
Image 3	62.8240	55.7069	12.8370	**111.2192**
Image 4	73.0443	66.1319	23.0579	**117.1331**
Image 5	64.3326	56.5960	14.3469	**111.2179**
Image 6	**53.9406**	28.0523	3.9771	33.5540
Image 7	59.7745	44.7221	9.8164	**70.5774**
Image 8	57.4528	37.8933	7.4725	**59.8518**
Image 9	**57.6666**	32.8618	7.6925	40.2024
Image10	**55.0038**	33.0128	5.0393	44.7346

As shown in Table 1, the mean values of the original images were relatively low (ranging from 53 to 73). The traditional linear grayscale enhancement method yielded limited improvement, and the gamma transformation method with $\gamma = 1$ even resulted in severely darkened images. In contrast, the image mean values processed by the proposed algorithm were significantly the highest (reaching up to 117.1331), indicating that the proposed algorithm can effectively enhance the overall brightness of low-light images and achieve the best brightness enhancement effect.

4.2 Image Standard Deviation Comparison

The image standard deviation reflects the dispersion degree of the pixel grayscale values in an image, directly reflecting the image contrast. A larger standard deviation indicates a broader grayscale distribution and higher contrast, whereas a smaller standard deviation implies lower contrast. Low-light images generally suffer from insufficient contrast. By comparing the standard deviations of images processed by different algorithms, the capability of each algorithm to enhance image contrast can be objectively evaluated.

Table 2. Image Standard Deviation Comparison

Image	Linear grayscale enhancement method	Gamma transformation method $\boldsymbol{\gamma = 0.5}$	Gamma transformation method $\boldsymbol{\gamma = 1}$	The proposed algorithm
Image 1	12.8170	25.9025	12.7980	**68.3001**
Image 2	9.5853	23.7301	9.5767	**67.7767**
Image 3	6.7835	15.2778	6.8773	**48.1831**
Image 4	22.6004	39.5288	22.5664	**85.9137**
Image 5	11.3858	22.7994	11.3870	**61.9628**
Image 6	6.3366	17.8562	6.3299	**44.0754**
Image 7	12.9862	24.0569	12.9629	**60.7863**
Image 8	9.5660	23.3862	9.5577	**56.6532**
Image 9	17.3546	31.9102	17.3444	**67.2987**
Image10	5.8309	16.8260	5.8164	**44.6833**

As shown in Table 2, the standard deviations of the original images were relatively low (ranging from 5.8 to 22.6). The standard deviations after processing by the linear grayscale enhancement method and the gamma transformation method ($\gamma = 1$) were almost identical to those of the original images, failing to effectively enhance the contrast. The gamma transformation method ($\gamma = 0.5$) provided a slight improvement. In contrast, the standard deviations of the images processed by the proposed algorithm were significantly the highest (reaching up to 85.9137), indicating that the proposed algorithm can greatly expand the grayscale dynamic range, achieving significantly superior contrast enhancement compared to the other algorithms.

4.3 Comparison of Image Information Entropy

Image information entropy reflects the amount of information contained in an image, directly manifesting the richness of image details. A larger entropy value indicates more abundant image details, whereas a smaller entropy value implies a lack of details. Low-light images generally suffer from low information entropy due to insufficient lighting. Therefore, by comparing the image information entropy processed by different algorithms, the capability of each algorithm to preserve and enhance image detail information can be objectively evaluated.

As shown in Table 3, the information entropy of the original images was relatively low (ranging from 3.22 to 5.35). The linear grayscale enhancement method and the gamma transformation method ($\gamma = 1$) yielded limited improvement, while the gamma transformation method ($\gamma = 0.5$) provided moderate improvement. In contrast, the proposed algorithm achieved the highest information entropy on the vast majority of images (reaching up to 6.6316), indicating that the proposed algorithm can effectively enrich image details while enhancing contrast. Its overall information retention capability is superior to the other comparison algorithms.

Table 3. Comparison of Image Information Entropy

Image	Linear grayscale enhancement method	Gamma transformation method $\gamma = 0.5$	Gamma transformation method $\gamma = 1$	The proposed algorithm
Image 1	4.7095	6.0227	4.5646	**6.1606**
Image 2	4.8288	6.0941	4.6667	**6.4671**
Image 3	4.6651	5.8173	4.6447	**6.3775**
Image 4	5.3550	**6.3455**	5.2436	5.7960
Image 5	5.1339	6.2137	5.0551	**6.6316**
Image 6	3.4914	5.1429	3.0972	**5.1493**
Image 7	4.1313	5.4386	4.1931	**5.5435**
Image 8	4.2501	5.7367	4.0135	**5.8010**
Image 9	3.2270	**4.0596**	2.7736	3.9536
Image10	3.8554	5.4240	3.5813	**5.5547**

4.4 Image NIQE Comparison

NIQE is utilized to evaluate the naturalness and overall quality of images. Unlike the previous three metrics, a lower NIQE value indicates smaller image distortion and a closer approximation to the natural state. Low-light images are highly prone to introducing noise and artifacts during the process of contrast enhancement. Therefore, this section evaluated the ability of each algorithm to maintain image naturalness while improving visual effects by comparing their NIQE values.

Table 4. Image NIQE Comparison

Image	Linear grayscale enhancement method	Gamma transformation method $\gamma = 0.5$	Gamma transformation method $\gamma = 1$	The proposed algorithm
Image 1	6.6459	**5.7395**	6.6103	6.6421
Image 2	**3.4504**	3.5425	3.4804	3.7317
Image 3	4.0594	**3.8397**	4.0446	4.2266
Image 4	3.7730	4.3164	**3.7669**	5.0056
Image 5	5.0353	4.8355	4.9939	**4.7548**
Image 6	**3.4138**	5.6928	3.4255	5.1051
Image 7	7.3453	7.7407	**7.3268**	7.6262
Image 8	4.7395	**2.7724**	2.7724	3.6152
Image 9	7.4623	5.7439	7.5963	**4.7677**
Image10	5.5649	**3.3072**	5.5822	3.5772

As shown in Table 4, the NIQE values of the original images were distributed between 3.45 and 7.46. The values of the linear grayscale enhancement method and the gamma transformation method ($\gamma = 1$) were basically on par with those of the original images. The gamma transformation method ($\gamma = 0.5$) yielded the lowest values on most images, exhibiting the best naturalness. The NIQE values of the proposed algorithm were at a moderate level. This is primarily because the algorithm significantly enhanced image brightness and contrast; when intensely stretching the grayscale dynamic range, it inevitably amplified local noise or introduced slight distortion, resulting in a slight decrease in naturalness. Overall, while significantly improving the overall visual effects and detail information of the images, the proposed algorithm still maintained an acceptable level of image naturalness, and its comprehensive enhancement performance remained outstanding.

5. CONCLUSION

In this paper, the Hopf bifurcation and 1:1 resonance characteristics of a class of time-delay neural network models were investigated and applied to low-contrast image enhancement. Theoretical

analysis demonstrated that under specific parameters, the system undergoes a 1:1 resonant Hopf bifurcation, and the amplitude of the periodic solution grows at a rate of $\mu^{\frac{1}{6}}$, providing a clear dynamical mechanism for signal amplification.

Based on this mechanism, an image enhancement algorithm was constructed, and experiments were conducted using 10 real low-light images from the LIME dataset. The proposed algorithm was compared with the linear grayscale enhancement method and the gamma transformation method. The results indicated that the proposed algorithm was significantly superior in terms of image mean, standard deviation, and information entropy, effectively improving image brightness, contrast, and detail richness. It performed moderately on the NIQE index, indicating a compromise in naturalness when intensely stretching the grayscale range; however, the comprehensive enhancement performance remained outstanding.

The proposed method provides a new approach with a clear mathematical mechanism for image enhancement. Future work will focus on the adaptive selection of the output moment, noise suppression, and integration with deep learning methods to further enhance the engineering practicality of the algorithm.

ACKNOWLEDGMENTS

Funding: This research is supported by the Undergraduate Innovation and Entrepreneurship Training Program of China University of Mining and Technology (Beijing) (Project No. 202514021).

REFERENCES

[1] Jain, A. (1989). Fundamentals of digital image processing. Computer Vision, Graphics, and Image Processing, 46(3), 400. https://doi.org/10.1016/0734-189x(89)90041-8

[2] Gonzalez, R. C., & Woods, R. E. (1980). Digital image processing. IEEE Transactions on Acoustics, Speech, and Signal Processing, 28(4), 484–486. https://doi.org/10.1109/TASSP.1980.1163437

[3] Ronneberger, O., Fischer, P., & Brox, T. (2015). U-Net: Convolutional networks for biomedical image segmentation. In N. Navab, J. Hornegger, W. M. Wells, & A. F. Frangi (Eds.), Medical image computing and computer-assisted intervention – MICCAI 2015 (pp. 234–241). Springer International Publishing.

[4] Canny, J. (1986). A computational approach to edge detection. IEEE Transactions on Pattern Analysis and Machine Intelligence, PAMI-8(6), 679–698. https://doi.org/10.1109/TPAMI.1986.4767851

[5] Long, J., Shelhamer, E., & Darrell, T. (2015). Fully convolutional networks for semantic segmentation. IEEE Transactions on Pattern Analysis and Machine Intelligence, 39(4), 640–651. https://doi.org/10.1109/CVPR.2015.7298965

[6] Dabov, K., Foi, A., Katkovnik, V., & Egiazarian, K. (2007). Image denoising by sparse 3-D transform-domain collaborative filtering. IEEE Transactions on Image Processing, 16(8), 2080–2095. https://doi.org/10.1109/TIP.2007.901238

[7] Krizhevsky, A., Sutskever, I., & Hinton, G. E. (2012). ImageNet classification with deep convolutional neural networks. In F. Pereira, C. J. C. Burges, L. Bottou, & K. Q. Weinberger (Eds.), Advances in neural information processing systems (Vol. 25). Curran Associates. https://doi.org/10.1145/3065386

[8] Goodfellow, I. J., Pouget-Abadie, J., Mirza, M., Xu, B., Warde-Farley, D., Ozair, S., Courville, A., & Bengio, Y. (2014). Generative adversarial nets. In Z. Ghahramani, M. Welling, C. Cortes, N. D. Lawrence, & K. Q. Weinberger (Eds.), Advances in neural information processing systems (Vol. 27). Curran Associates.

[9] Morfu, S., & Comte, J. C. (2004). A nonlinear oscillators network devoted to image processing. International Journal of Bifurcation and Chaos, 14(4), 1385–1394. https://doi.org/10.1142/S0218127404009879

[10] Morfu, S., Bossu, J., & Marquié, P. (2006). Contrast enhancement with a nonlinear oscillators network. Nonlinear Dynamics, 44(1–4), 173–180. https://doi.org/10.1007/s11071-006-1964-y

[11] Morfu, S. (2009). On some applications of diffusion processes for image processing. Physics Letters A, 373(29), 2438–2444. https://doi.org/10.1016/j.physleta.2009.04.076

[12] Wen, L., Wang, L., & Xu, Y. (2019). Bifurcation of a feed forward neural network with delay and application in image contrast enhancement. Mathematical Biosciences and Engineering, 17(1), 387–403. https://doi.org/10.3934/mbe.2020021

[13] McCullen, N. J., Mullin, T., & Golubitsky, M. (2007). Sensitive signal detection using a feed-forward oscillator network. Physical Review Letters, 98(25), 254101. https://doi.org/10.1103/PhysRevLett.98.254101

[14] Postlethwaite, C., & Golubitsky, M. (2012). Feed-forward networks, center manifolds, and forcing. Discrete & Continuous Dynamical Systems, 32(8), 2913–2935. https://doi.org/10.3934/dcds.2012.32.2913

[15] Ruan, S., & Wei, J. (2003). On the zeros of transcendental functions with applications to stability of delay differential equations with two delays. Dynamics of Continuous, Discrete and Impulsive Systems, 10(6), 863–874. https://doi.org/10.1093/imammb/18.1.41

[16] Wang, W., Lin, X., & Zhang, C. (2021). Resonant bifurcation of feed-forward chains and application in image contrast enhancement. Mathematics and Computers in Simulation, 187, 410–425. https://doi.org/10.1016/j.matcom.2021.03.004

[17] Wang, Z., Bovik, A. C., Sheikh, H. R., & Simoncelli, E. P. (2011). Perceptual visual quality metrics: A survey. Journal of Visual Communication and Image Representation, 22(4), 297–312. https://doi.org/10.1016/j.jvcir.2011.01.005